On Performance of Fluid Antenna System using Maximum Ratio Combining

Xiazhi Lai, Tuo Wu, Junteng Yao, Cunhua Pan, *Senior Member, IEEE*, Maged Elkashlan, *Senior Member, IEEE*, and Kai-Kit Wong, *Fellow, IEEE*

***Abstract*—This letter investigates a fluid antenna system (FAS) where multiple ports can be activated for signal combining for enhanced receiver performance. Given M ports at the FAS, the best K ports out of the M available ports are selected before maximum ratio combining (MRC) is used to combine the received signals from the selected ports. The aim of this letter is to study the achievable performance of FAS when more than one ports can be activated. We do so by analyzing the outage probability of this setup in Rayleigh fading channels through the utilization of Laplace transform, lower bound estimation, and high signal-to-noise ratio (SNR) asymptotic approximations. Our analytical results demonstrate that FAS can harness rich spatial diversity, which is confirmed by computer simulations.**

***Index Terms*—Diversity, fluid antenna system (FAS), maximum ratio combining (MRC), outage probability.**

I. Introduction

Fluid antenna systems (FASs) capitalize upon the inherent spatial diversity by dynamically adjusting the antenna elements to optimal positions, referred to as "ports". This new paradigm stands in contrast to traditional communication methodologies, in which the antenna elements remain in fixed positions, as elucidated by Shojaeifard *et al.* in [1]. The realization of FAS may come in the forms of liquid-metal-based antennas [2] or on-off pixel-based antennas [3]. See [4] for more details.

Motivated by the great potential of FAS, recent research has delved into the FAS channel model, deriving the probability density function (PDF) of the received signal-to-noise ratio (SNR) as well as the corresponding outage probability [5], [6], [7]. Remarkably, the outcomes of their investigation unveiled the superiority of FAS over conventional fixed-position antenna systems. Machine learning techniques have also been proposed for port selection in FAS [8]. Most recently, Wong *et al.* has extended the use of FAS for multiple access by taking advantage of the ups and downs of fading channels in the spatial domain, and illustrated the possibility of alternative multiple access schemes using FAS [9], [10], [11].

However, research in FAS is still in an early stage and the majority of the results so far are limited to FAS with only one selected port exhibiting the maximum SNR [5], [6], [7], [8], [9], [10]. The fact that a 5G mobile terminal is required to have more than one radio frequency (RF) chains means that FAS is expected to come with multiple activated ports for better performance [12]. As maximum ratio combining (MRC) is the optimal mixing scheme without interference, it is therefore of great importance to understand the achievable performance of FAS using MRC if more than one ports can be selected.

Specifically, our contributions are summarized as follows:

- First, we consider a K-port FAS which corresponds to a FAS with K selected ports, operating in Rayleigh fading channels. The mobile receiver selectively activates the K optimal ports from the available M ports. Then MRC is employed to combine the K branches of signals from the activated ports. We derive the outage probability of the system using the Laplace transform (LT) method.
- Additionally, we present the lower bound and asymptotic expressions for the outage probability.
- The simulation results substantiate the effectiveness of the proposed analytical approach, thereby confirming and validating our insights and discussions.

II. System Model

Consider an end-to-end communication in Rayleigh fading channels, where the source transmits the signal using a conventional fixed-position antenna with transmit power P_S but the receiver is equipped with a FAS with K fluid antenna elements.[1] Each antenna element is connected to one RF chain. Within this particular FAS configuration, a linear space of $W\lambda$ encompasses a total of M ports, where λ represents the wavelength. [5]. Among these M ports, it is assumed that each port is evenly distributed, and K ports can be activated and are connected to the RF chains for signal reception.

Since each port is placed closely, the channel parameters of each port are correlated. Building upon the channel model developed in [7] and [10], we introduce a virtual reference port to model the channel correlation. This virtual reference port is characterized by a channel parameter $h_0 \sim \mathcal{CN}(0, \alpha)$, following a complex Gaussian distribution with zero mean and variance α. Accordingly, the SNR of h_0 can be written as

$$\gamma_0 = \frac{P_S|h_0|^2}{\sigma^2}, \tag{1}$$

where σ^2 denotes the noise power level. Considering h_0 as a complex Gaussian random variable (RV), the PDF of γ_0 can

(Corresponding authors: Tuo Wu, Cunhua Pan and Kai-Kit Wong.)

X. Lai is with the School of Computer Science, Guangdong University of Education, Guangzhou, Guangdong, China (E-mail: xzlai@outlook.com).

T. Wu and M. Elkashlan are with the School of Electronic Engineering and Computer Science at Queen Mary University of London, London E1 4NS, U.K. (Email:{tuo.wu, maged.elkashlan}@qmul.ac.uk).

J. Yao is with the Faculty of Electrical Engineering and Computer Science, Ningbo University, Ningbo 315211, China (E-mail: juntengyao512@163.com).

C. Pan is with the National Mobile Communications Research Laboratory, Southeast University, Nanjing 210096, China. (e-mail: cpan@seu.edu.cn).

K. K. Wong is with the Department of Electronic and Electrical Engineering, University College London, WC1E 6BT London, U.K., and also with the Yonsei Frontier Laboratory and the School of Integrated Technology, Yonsei University, Seoul 03722, South Korea (e-mail: kat-kit.wong@ucl.ac.uk).

[1] In our idealized mathematical model, a FAS with multiple single-activated-port fluid antennas is equivalent to a FAS with multiple activated ports although their specific implementation details will differ.

be expressed as

$$f_{\gamma_0}(x) = \frac{1}{\phi} e^{-\frac{x}{\phi}}, \tag{2}$$

where $\phi = P_S\alpha/\sigma^2$ represents the average received SNR. Now, we proceed to establish the channel parameter linking the source and the m-th port, denoted as h_m, where $m \in \mathcal{M} = \{1, 2, \ldots, M\}$. The expression for h_m takes the form

$$h_m = \sqrt{\mu} h_0 + \sqrt{1-\mu} e_m, \tag{3}$$

where $e_m \sim \mathcal{CN}(0, \alpha)$ for $m \in \mathcal{M}$ are independently and identically distributed (i.i.d.) RVs, α is the average channel gain from the source to the ports. Additionally, μ denotes the correlation factor, which is given by [7]

$$\mu = \sqrt{2}\sqrt{{}_1F_2\left(\frac{1}{2}; 1; \frac{3}{2}; -\pi^2 W^2\right) - \frac{J_1(2\pi W)}{2\pi W}}, \tag{4}$$

where ${}_aF_b$ denotes the generalized hypergeometric function and $J_1(\cdot)$ is the first-order Bessel function of the first kind.[2]

Conditioned on a fixed channel parameter h_0, and in accordance with γ_0, the corresponding SNR of h_m, expressed as $\gamma_m = \frac{P_S |h_m|^2}{\sigma^2}$, follows a non-central chi-square distribution. The conditional PDF can be expressed as [14]

$$f_{\gamma_m|\gamma_0 = x_0}(x) = \omega e^{-\omega(x+\mu x_0)} I_0\left(2\omega\sqrt{\mu x_0 x}\right), \tag{5}$$

where $\omega = \left(\phi(1-\mu)\right)^{-1}$. Besides, $I_0(u)$ is the modified Bessel function of the first kind with order 0, which can be expressed in series representation as [18]

$$I_0(z) = \sum_{k=0}^{\infty} \frac{z^{2k}}{2^{2k} k! \Gamma(k+1)}. \tag{6}$$

Combining (5) with (6), we further derive $f_{\gamma_m|\gamma_0=x_0}(x)$ as

$$f_{\gamma_m|\gamma_0=x_0}(x) = \sum_{k=0}^{\infty} c_k x_0^k e^{-\omega\mu x_0} x^k e^{-\omega x}, \tag{7}$$

where

$$c_k = \frac{\omega^{2k+1}\mu^k}{(k!)^2}. \tag{8}$$

In order to receive the signal transmitted from the source, the receiver selects the K ports with the K highest received SNR from the available total of M ports for activation. The set of selected ports is denoted by $\mathbb{K}$. In addition, to process the received signals from different antenna elements, the MRC technique is utilized to combine the K branches of signals.[3]

[2]In the case of rich scattering, the most accurate channel model for the analysis of FAS appears to be the one in [13]. However, as shown in [13], performance analysis based on that model is hardly tractable, not to mention if MRC is considered in conjunction with port selection in FAS. As a remedy, the model in [7], which considers the compound correlation effect from all ports, is preferred here to keep the tractability. The discrepancies between this model and other models have been discussed in [10] and it was shown that the simplified model is accurate if the SNR threshold is not so large.

[3]The proposed combining technique resembles the generalized selection combining technique [15], [16], which has been applied to process the signal combining of multiple-antenna systems, and several works on the performance of independent paths have been reported in the literature [17]. However, for the proposed FAS using MRC, our distinctive contribution is to deduce the outage probability considering the effect of correlation among the ports.

Moreover, the channel state information (CSI) is assumed to be not available at the source; hence the transmission data rate is fixed to R. Therefore, the outage of communication occurs when the FAS cannot sustain the data rate R, i.e.,

$$\mathcal{E} = \left\{\log_2\left(1 + \sum_{m\in\mathbb{K}} \gamma_m\right) \le R\right\}. \tag{9}$$

Thus, the system's outage probability is written as

$$P_{\text{out}} = \Pr\left(\mathcal{E}\right). \tag{10}$$

III. Performance Analysis

Here, we derive the exact outage probability of the proposed FAS-enabled communications. Subsequently, the lower bound and asymptotic expressions of the outage probability of the FAS are derived. These derivations offer valuable insights for the proposed FAS-enabled communications system.

A. Exact Outage Probability

Denote the outage probability conditioned on $\gamma_0 = x_0$ as

$$\Lambda(z) = \Pr\left(\sum_{m\in\mathbb{K}} \gamma_m \le z | \gamma_0 = x_0\right). \tag{11}$$

Then taking the expectation over RV γ_0 into (11), the system outage probability can be obtained. The calculation of $\Lambda(z)$ can be conducted by considering the fact that γ_m for $m \in \mathcal{M}$ are i.i.d. RVs with fixed $\gamma_0 = x_0$ and the following two cases:

Case 1: When $M > K$, we can calculate $\Lambda(z)$ as follows.

Consider the port with the $(K+1)$-th maximal channel gain, denoted as v. Given $\gamma_{K+1} = v$, we can derive the probability that the channel gains of the last $T = M - K - 1$ ports are smaller than v as

$$\Psi(v, x_0) = \Pr\left(\gamma_m \le v, m \in \mathcal{T} | \gamma_0 = x_0\right), \tag{12}$$

where $\mathcal{T} = \{K+2, K+3, \ldots, M\}$. Moreover, the probability that the first K ports are selected and outage occurs is given by

$$\Phi(z, v, x_0) = \Pr\left(\sum_{m\in\mathcal{K}} \gamma_m \le z, \gamma_m > v | \gamma_0 = x_0\right), \tag{13}$$

where $\mathcal{K} = \{1, 2, \ldots, K\}$ and $z = 2^R - 1$ denotes the SNR threshold of outage.

Different combinations can be made with the selected ports, especially concerning the port with the $(K+1)$-th maximal channel gain. The outage probability, when this gain is v and when γ_0 is set to x_0, is given by $\binom{M}{K}(T+1)\Phi(z, v, x_0)\Psi(v, x_0)$. This is because, out of M ports, K are chosen for MRC, leaving the $(K+1)$-th maximal gain port to be considered among the remaining $T+1$ ports. By computing the expectation of $\binom{M}{K}(T+1)\Phi(z, v, x_0)\Psi(v, x_0)$ with respect to v, we derive $\Lambda(z)$ as

$$\Lambda(z) = \binom{M}{K}(T+1)\int_0^{\infty} \Phi(z, v, x_0)\Psi(v, x_0) f_{v|\gamma_0=x_0}(v) dv. \tag{14}$$

Case 2: When $M = K$, all ports are activated, we have $\Lambda(z) = \Phi(z, 0, x_0)$.

In the following, we derive the expressions of $\Psi(v, x_0)$ and $\Phi(z, v, x_0)$. Then we obtain the outage probability by taking the expectation of $\Lambda(z)$ with respect to γ_0.

First, it is important to note that $\forall m, l \in \mathcal{T}$, γ_m and γ_l are independent with each other given $\gamma_0 = x_0$. Furthermore, in accordance with (5), the joint PDF of γ_m for $m \in \mathcal{T}$ can be expressed as

$$\begin{aligned} &f_{\gamma_m, m\in\mathcal{T}|\gamma_0=x_0}(x_1, \ldots, x_T) \\ &\quad = \prod_{m=1}^{T} \omega e^{-\omega(x_m+\mu x_0)} I_0\big(2\omega\sqrt{\mu x_0 x_m}\big). \end{aligned} \tag{15}$$

Then, by utilizing (12) and (15), we evaluate $\Psi(v, x_0)$ as

$$\begin{aligned} \Psi(v, x_0) &= \int_0^v \cdots \int_0^v f_{\gamma_m, m\in\mathcal{T}|\gamma_0=x_0}(x_1, \ldots, x_T) dx_1 \cdots dx_T \\ &= \Big(1 - Q_1\big(\sqrt{2\omega\mu x_0}, \sqrt{2\omega v}\big)\Big)^T, \end{aligned} \tag{16}$$

where $Q_1(\cdot,\cdot)$ is the first order Marcum-Q function [6].

Next, we proceed to derive the analytical expression of $\Phi(z, v, x_0)$ by utilizing the following theorem.

Theorem 1: The LT expressions of the following functions

$$g(x) = x^a e^{-bx} u(x - v), \tag{17}$$
$$p(x) = (x - a)^{K-1} e^{-bx} u(x - a), \tag{18}$$

are, respectively,

$$L[g(x); s] = e^{-(s+b)v} \sum_{l=0}^{a} \frac{a! v^l}{l!(s+b)^{a+1-l}}, \tag{19}$$
$$L[p(x); s] = \frac{(K-1)! e^{-a(s+b)}}{(s+b)^K}, \tag{20}$$

where $\mathrm{Re}(s) \geq -b$, Re(x) denotes the real part of x, and $u(\cdot)$ is the step function.

Proof: See Appendix A. ■

From Theorem 1 and (7), the LT of the PDF of γ_m with $\gamma_m > v$ is given by

$$\begin{aligned} &L\big[f_{\gamma_m|\gamma_0=x_0}(x_m); s\big] \\ &\quad = e^{-(s+\omega)v-\omega\mu x_0} \sum_{m=0}^{\infty} \sum_{l=0}^{m} \frac{d_m x_0^m v^l}{l!(s+\omega)^{m+1-l}}, \end{aligned} \tag{21}$$

where Re(s) $\geq -\omega$ and $d_m = c_m m!$.

Then, by using the faltung theorem in [18], the LT of the PDF of RV $\bar{\gamma} = \sum_{m\in\mathcal{K}} \gamma_m$ conditioned on $\gamma_m > v$ can be derived as

$$\begin{aligned} L\big[f_{\bar{\gamma}|\gamma_0=x_0}(x); s\big] &= \Big(L\big[f_{\gamma_m|\gamma_0=x_0}(x_m); s\big]\Big)^K \\ &= e^{-Kv(s+\omega)-K\omega\mu x_0} \sum_{\substack{r_m=0\\ m\in\mathcal{K}}}^{\infty} \rho_m x_0^{\eta_m} \sum_{\substack{l_m=0\\ m\in\mathcal{K}}}^{r_m} \frac{v^{\epsilon_m} q_m}{(s+\omega)^{\chi_m}}, \end{aligned} \tag{22}$$

where $\rho_m = \prod_{m=1}^{K} d_m$, $\eta_m = \sum_{m=1}^{K} r_m$, $\epsilon_m = \sum_{m=1}^{K} l_m$, $q_m = \prod_{m=1}^{K} \frac{1}{l_m!}$, and $\chi_m = K + \eta_m - \epsilon_m$. Utilizing Theorem 1, we can obtain the PDF of $\bar{\gamma}$ conditioned on $\gamma_0 = x_0$ as

$$\begin{aligned} f_{\bar{\gamma}|\gamma_0=x_0}(x) &= e^{-\omega(x+K\mu x_0)} \sum_{\substack{r_m=0\\ m\in\mathcal{K}}}^{\infty} \rho_m x_0^{\eta_m} \\ &\quad \times \sum_{\substack{l_m=0\\ m\in\mathcal{K}}}^{r_m} v^{\epsilon_m} q_m \frac{(x-Kv)^{\chi_m-1}}{(\chi_m-1)!}, \end{aligned} \tag{23}$$

with $x \geq Kv$. Based on (23), the computation of $\Phi(z, v, x_0)$ can be performed by

$$\begin{aligned} \Phi(z, v, x_0) &= \int_{Kv}^{z} f_{\bar{\gamma}|\gamma_0=x_0}(x) dx = e^{-\omega(Kv+K\mu x_0)} \times \\ &\sum_{\substack{r_m=0\\ m\in\mathcal{K}}}^{\infty} \rho_m x_0^{\eta_m} \times \sum_{\substack{l_m=0\\ m\in\mathcal{K}}}^{r_m} v^{\epsilon_m} q_m \frac{\gamma\big(\chi_m, \omega(z-Kv)\big)}{(\chi_m-1)!\,\omega^{\chi_m}}, \end{aligned} \tag{24}$$

in which $z \geq Kv$ is a necessary condition; otherwise, $\Phi(z, v, x_0) = 0$. In addition, $\gamma(\alpha, x)$ is the lower incomplete Gamma function, which can be expressed in integral and serial representations respectively, as

$$\gamma(\kappa, x) = \int_0^x e^{-t} t^{\kappa-1} dt = (\kappa-1)! \left(1 - e^{-x} \sum_{m=0}^{\kappa-1} \frac{x^m}{m!}\right). \tag{25}$$

Calculating $\Lambda(z)$ in (11) with (16) and (24), and then taking the expectation of $\Lambda(z)$ with respect to γ_0, the outage probability of the system can be computed as

$$P_{\rm out} = \begin{cases} P_{\rm out,1}, & M > K, \\ P_{\rm out,2}, & M = K, \end{cases} \tag{26}$$

where

$$\begin{aligned} P_{\rm out,1} = \int_0^{\infty} \int_0^{\frac{z}{K}} &\binom{M}{K} (T+1) \Phi(z, v, x_0) \Psi(v, x_0) \\ &\times f_{\gamma_m|\gamma_0=x_0}(v) f_{\gamma_0}(x_0) dv dx_0, \end{aligned} \tag{27}$$

and

$$\begin{aligned} P_{\rm out,2} &= \int_0^{\infty} \Phi(z, 0, x_0) f_{\gamma_0}(x_0) dx_0 \\ &= \sum_{\substack{r_m=0\\ m\in\mathcal{K}}}^{\infty} \frac{\eta_m! \rho_m \gamma\big(K+\eta_m, \omega z\big)}{(K+\eta_m-1)!\,\omega^{K+\eta_m} (\omega K\mu)^{\eta_m+1}}. \end{aligned} \tag{28}$$

Remark 1: From (16), it becomes evident that $\Psi(v, x_0)$ becomes tiny with a large value of T, owing to the fact that $Q_1(\cdot,\cdot)$ is bounded by 1 [6]. This observation implies that $P_{\rm out}$ in (26), i.e., the outage probability of the system approaches zero when the total number of ports $M \to \infty$.[4]

[4]Note that the conclusion may vary depending on how spatial correlation over the ports is modelled. That said, the analysis presented in this letter gives the first-look performance of FAS using MRC.

B. Lower Bound and Asymptotic Analysis

For the sake of facilitating computation and analysis of P_{out}, we derive a lower bound for $P_{\text{out},1}$ in this subsection. Notably, this lower bound closely approximates the exact outage probability, particularly in the high SNR region. Moreover, we analyze the asymptotic behavior of P_{out} and discuss the performance bottleneck of the system.

First, from (7), we can readily know that $f_{\gamma_m|\gamma_0=x_0}(x)$ is lower-bounded by

$$\bar{f}_{\gamma_m|\gamma_0=x_0}(x) = \omega e^{-\omega\mu x_0} e^{-\omega x}. \tag{29}$$

Based on (29), we can accordingly obtain the lower bound of $\Psi(v, x_0)$ and $\Phi(z, v, x_0)$, respectively, as

$$\bar{\Psi}(v, x_0) = e^{-\omega T \mu x_0} \sum_{t=0}^{T} \binom{T}{t} (-1)^t e^{-\omega t v}, \tag{30}$$

$$\bar{\Phi}(z, v, x_0) = e^{-\omega(Kv + K\mu x_0)} - e^{-\omega(z + K\mu x_0)} \times \sum_{k=0}^{K-1} \frac{\omega^k}{k!} \sum_{m=0}^{k} \binom{k}{m} z^{k-m} (-Kv)^k. \tag{31}$$

Applying (29)–(31) into (27), we can obtain

$$P_{\text{out},1} \geq \bar{P}_{\text{out},1} = \binom{M}{K} \frac{T+1}{M\mu\omega\phi + 1} \times \left(\sum_{t=0}^{T} \binom{T}{t} \beta_t - \sum_{t=0}^{T} \sum_{k=0}^{K-1} \sum_{m=0}^{k} \binom{T}{t} \binom{k}{m} \kappa_{t,k,m} \right), \tag{32}$$

where

$$\beta_t = \frac{(-1)^t}{(t+K+1)} \left(1 - e^{-z\omega(t+K+1)}\right), \tag{33}$$

$$\kappa_{t,k,m} = \frac{(-1)^{t+m} K^m (z\omega)^{k-m} \gamma\left(m+1, \frac{z\omega(t+1)}{K}\right)}{k!(t+1)^{m+1}}. \tag{34}$$

From (7), it becomes apparent that the exact value of $P_{\text{out},1}$ approaches the lower bound $\bar{P}_{\text{out},1}$ as the average received SNR becomes large, i.e., the values of α or P_S are large. Moreover, when the value of M and K are large, the calculations of outage probabilities $P_{\text{out},1}$ in (27) become intricate. In contrast, the evaluation of $\bar{P}_{\text{out},1}$ using the expression in (32) remains computationally efficient, aiding in the analysis of the performance of the proposed system.

Furthermore, by applying the expansion $e^{-x} = 1 - x$ for tiny value of $|x|$, we can obtain the asymptotic expression of outage probability in the high SNR region as

$$P_{\text{out}} \simeq \psi (z\omega)^M, \tag{35}$$

where

$$\psi = \begin{cases} \binom{M}{K} \frac{(T+1)(1-\mu)}{K!(M\mu - \mu + 1)K^{T+1}} \times \sum_{k=0}^{K} \binom{K}{k} \frac{(-1)^k}{k+T+1}, & M > K, \\ \frac{1-\mu}{M!(M\mu - \mu + 1)}, & M = K. \end{cases} \tag{36}$$

The asymptotic outage probability in (35) indicates that the diversity order of the FAS-aided communication system is M, which is consistent to the result for the independent channel model with selection combining or MRC.

IV. Numerical Results

Here, we present numerical results for the FAS-aided communications. Following a similar approach in [7], we assume the value of $W = 0.4$. Also, we set the data rate R to 4 bit/s/Hz, with an outage SNR threshold $z = 15$. Unless specified otherwise, we refer to the outcomes of our simulations as “Simul”. We numerically evaluate the integral (26) using Gauss-Chebyshev quadrature with the 100 grid points for each dimension [19]. Also, we denote the results obtained from (26), (32), and (35) as “Ana.”, “LB”, and “Asy.”, respectively.

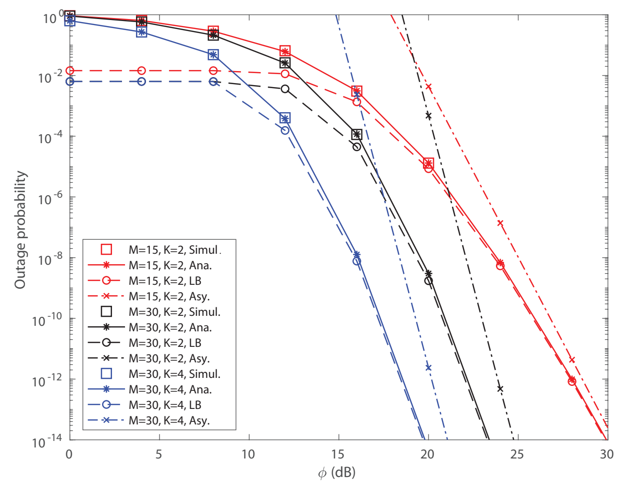

Fig. 1. Outage probability versus average SNR ϕ.

Fig. 1 shows the variations in outage probability with the average SNR (ϕ), considering different values of M and K. As seen from Fig. 1, the analytical outage probability derived from (26) closely aligns with the simulation results. Additionally, the lower bound provided by (32) accurately approximates the simulation outcomes, particularly in the high SNR region, which corroborates with the asymptotic result in (35).

Furthermore, Fig. 1 indicates that the outage probability is mainly influenced by the total port number M, affirming the analysis in (35) that the diversity stemming from all available ports can be maximally exploited. It is worth noting that the gain achieved by increasing K from 2 to 4 in the high SNR region is approximately 3.8, consistent with the findings presented in (35). However, the enhancement resulting from increasing the number of activated ports K is comparatively less pronounced than the gains derived from increasing M.

Fig. 2 provides a visualization of the relationship between the number of activated ports (K) and the resulting outage probability in the context of the K-port FAS-aided communications system. The simulations were conducted with ϕ set at 15 dB, and two distinct values for the total port count (M), namely 15 and 30. Meanwhile, the number of activated ports K is allowed to vary from 1 to 6. For comparison, the results of random port selection with MRC scheme are provided as

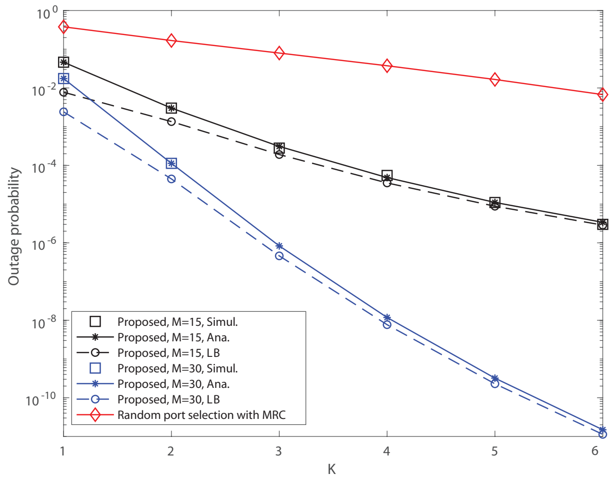

Fig. 2. Outage probability versus number of antenna elements K.

well. As observed, the lower bound is not quite accurate for small values of K. Also, the proposed scheme significantly outperforms the random port selection with MRC.

Upon examining the results depicted in Fig. 2, it becomes evident that increasing the count of activated ports (K) contributes significantly to enhancing the overall system's outage performance. Nevertheless, the most striking insight emerges from the clear trend indicating that the advantages stemming from augmenting the total port count (M) are even more pronounced. This noteworthy pattern is in concordance with the analytical findings presented in the preceding sections.

V. Conclusion

This letter attempted to analyze the FAS-aided communications system with multiple activated ports, where the MRC technique was utilized to combine the signal from different activated ports. The outage probability of the proposed system has been derived in Rayleigh fading channels, in forms of exact expression, lower bound, and asymptotic expression. Analysis showed that the diversity order of the system equals the number of total available ports. Simulation results corroborated the effectiveness of the provided analysis.

Appendix A
Proof of Theorem 1

According to the definition of LT, we can compute the LT expression of $g(x)$ in (17) as

$$\begin{aligned} L[g(x);s] &= \int_0^\infty g(x)e^{-sx}dx = \int_v^\infty x^a e^{-(s+b)x}dx \\ &= e^{-(s+b)v}\sum_{l=0}^{a}\frac{a!v^l}{l!(s+b)^{a+1-l}}, \end{aligned} \tag{37}$$

where $\mathrm{Re}(s) \geq -b$, and the last step can be derived by using the partial integral technique.

Similarly, we can compute the LT expression of $p(x)$ as

$$\begin{aligned} L[p(x);s] &= \int_0^\infty p(x)e^{-sx}dx \\ &= \int_a^\infty (x-a)^{K-1}e^{-(b+s)x}dx \\ &\overset{(e_1)}{=} \frac{e^{-a(s+b)}}{(s+b)^K}\int_0^\infty t^{K-1}e^{-t}dt \\ &\overset{(e_2)}{=} \frac{(K-1)!e^{-a(s+b)}}{(s+b)^K}, \end{aligned} \tag{38}$$

where $\mathrm{Re}(s) \geq -b$, the step (e_1) can be obtained by setting $t = (x-a)(s+b)$, and step (e_2) uses the partial integral technique.

References

[1] A. Shojaeifard et al., "MIMO evolution beyond 5G through reconfigurable intelligent surfaces and fluid antenna systems," *Proc. IEEE*, vol. 110, no. 9, pp. 1244–1265, Sept. 2022.

[2] Y. Huang, L. Xing, C. Song, S. Wang, and F. Elhouni, "Liquid antennas: Past, present and future," *IEEE Open J. Antennas Propag.*, vol. 2, pp. 473–487, 2021.

[3] D. Rodrigo, B. A. Cetiner, and L. Jofre, "Frequency, radiation pattern and polarization reconfigurable antenna using a parasitic pixel layer," *IEEE Trans. Antennas Propag.*, vol. 62, no. 6, pp. 3422–3427, Jun. 2014.

[4] K. K. Wong, K. F. Tong, Y. Shen, Y. Chen, and Y. Zhang, "Bruce Lee-inspired fluid antenna system: Six research topics and the potentials for 6G," *Frontiers Commun. Netw., section Wireless Commun.*, 3:853416, Mar. 2022.

[5] K.-K. Wong, A. Shojaeifard, K.-F. Tong and Y. Zhang, "Performance limits of fluid antenna systems," *IEEE Commun. Letters*, vol. 24, no. 11, pp. 2469–2472, Nov. 2020.

[6] K.-K. Wong, A. Shojaeifard, K.-F. Tong, and Y. Zhang, "Fluid antenna systems," *IEEE Trans. Wireless Commun.*, vol. 20, no. 3, pp. 1950–1962, March 2021.

[7] K.-K. Wong, K. F. Tong, Y. Chen, and Y. Zhang, "Closed-form expressions for spatial correlation parameters for performance analysis of fluid antenna systems," *IET Electron. Lett.*, vol. 58, no. 11, pp. 454–457, May 2022.

[8] Z. Chai, K.-K. Wong, K.-F. Tong, Y. Chen, and Y. Zhang, "Port selection for fluid antenna systems," *IEEE Commun. Lett.*, vol. 26, no. 5, pp. 1180–1184, May 2022.

[9] K.-K. Wong and K.-F. Tong, "Fluid antenna multiple access," *IEEE Trans. Wireless Commun.*, vol. 21, no. 7, pp. 4801-C4815, Jul. 2022.

[10] K.-K. Wong, D. Morales-Jimenez, K.-F. Tong, and C.-B. Chae, "Slow fluid antenna multiple access," *IEEE Trans. Commun.*, vol. 71, no. 5, pp. 2831–2846, May 2023.

[11] N. Waqar, K.-K. Wong, K.-F. Tong, A. Sharples, and Y. Zhang, "Deep learning enabled slow fluid antenna multiple access," *IEEE Commun. Lett.*, vol. 27, no. 3, pp. 861–865, March 2023.

[12] K.-K. Wong, K.-F. Tong, and C.-B. Chae, "Fluid antenna system-part II: Research opportunities," *IEEE Commun. Lett.*, vol. 27, no. 8, pp. 1924–1928, Aug. 2023.

[13] M. Khammassi, A. Kammoun and M. -S. Alouini, "A new analytical approximation of the fluid antenna system channel," *IEEE Trans. Wireless Commun.*, doi: 10.1109/TWC.2023.3266411.

[14] M. K. Simon and M. Alouini, *Digital Communication over Fading Channels, 2nd ed.* New York: Wiley, 2005.

[15] T. Eng, N. Kong, and L. B. Milstein, "Comparison of diversity combining techniques for Rayleigh-fading channels," *IEEE Trans. Commun.*, vol. 44, pp. 1117–1129, Sept. 1996.

[16] M. Win and J. Winters, "Analysis of hybrid selection/maximal-ratio combining in Rayleigh fading," *IEEE Trans. Commun.*, vol. 47, no. 12, pp. 1773–1776, Dec. 1999.

[17] M. K. Simon and M. Alouini, "A compact performance analysis of generalized selection combining with independent but nonidentically distributed rayleigh fading paths," *IEEE Trans. Commun.*, vol. 50, no. 9, pp.1409–1412, Sept. 2002.

[18] I. S. Gradshteyn and I. M. Ryzhik, *Table of Integrals, Series, and Products, 7th ed.* San Diego, CA: Academic, 2007.

[19] E. Suli and D. F. Mayers, *An Introduction to Numerical Ananlysis*. Cambridge, U.K.: Cambridge Univ. Press, 2003.